LATVIAN JOURNAL OF PHYSICS AND TECHNICAL SCIENCES
2016, N 1

DOI: 10.1515/lpts-2016-0003

SMOOTH TRACKING TRAJECTORY GENERATION OF LARGE ANTENNA

S. Upnere*, N. Jekabsons, U. Locans

Ventspils University College,
101 Inženieru Str., Ventspils, LV – 3601, LATVIA
*Corresponding author: sabineu@venta.lv

The current paper presents an engineering approach for studies of the control algorithm designed for a mechanically robust large antenna. Feed-forward control methods with the 3rd-order polynomial tracking algorithm are supplemented to the original feed-back PID control system. Dynamical model of the existing servo system of 32m radio telescope has been developed to widen a case analysis of observation sessions and efficiency of the control algorithms due to limited access to an antenna. Algorithms along with the results from the system implemented on a real antenna as well as model results are presented.

Keywords: *dynamical model, path planning, PID controller, tracking algorithm.*

1. INTRODUCTION

The control systems of antennas and telescopes ensure accurate pointing (reaching the target object) and tracking (following the object during its apparent motion). Pointing and tracking are constrained by existing technical parameters of the drive system and mechanical properties of the whole construction (such as maximum motor torque, system acceleration and velocity), as well as by the choice of antenna control algorithms. Resultant accuracy and agility of a pointing and tracking system often limit the performance of the antenna.

There are several algorithms available that provide the control of antennas and telescopes. Proportional-Integral (PI) and Proportional-Integral-Derivative (PID) controller can be regarded as a classical approach in the antenna industry [1]. Over the last decades, a number of PID design methods have been proposed [2], [3], [4]. For PID controllers, windup is a characteristic feature; therefore, several anti-windup controller design methods have been proposed to suppress windup degradation ([5], [6], [7]).

Model-based design methods are often employed by control engineers and researchers. There have been several studies of model-based controllers applicable to the control system of the antenna and telescope, such as linear-quadratic-Gaussian [8] or H∞ controller [9]. Gawronski and Souccar have performed the analysis of the

effectiveness of different controller combinations in one system [1].

The transient response of a practical control system with a plant often exhibits damped oscillations before reaching a steady state [3]. One of transient response characteristics is settling time. It is the time required for a response curve to reach and stay within a range about the final value of size specified by absolute percentage of the final value [3]. There are references available which describe various approaches how to reduce overshoots before reaching a steady state. For example, one can change controller coefficients [10] or change planning of movement trajectory using the 5th-order polynomial [11] or the 3rd-order polynomial [12].

In general, there are two options that improve the efficiency of a tracking algorithm: feed-forward control and feed-back corrections. In this paper, we present the combined approach using the 3rd-order trajectory generation algorithm and PID controller to advance antenna switching between sources during the observation session. The objective of this study is the development of an additional feed-forward algorithm for existing PID controller of the antenna in terms of requirements for high accuracy observations and without changes in hardware. The used algorithm provides the desired position, velocity and acceleration limits, permitting their use in control to improve the tracking accuracy at all points on the path.

In order to check a tracking algorithm, the radio telescope RT-32 of Ventspils International Radio Astronomy Centre (VIRAC) located in Irbene (Latvia) has been used. The dish size of the fully steerable radio telescope RT-32 is 32 meters. Several experiments with different control algorithms have been performed using RT-32. However, real observations are a rather slow process; thus, this approach somehow limits a feasible number of pointing and tracking scenarios for controller evaluation. Thus, additional models of RT-32 servo system have been developed. Mechanical and kinematic models of existing RT-32 drive system have been used for optimal movement planning during the Very Long Baseline Interferometry (VLBI) sessions or satellite tracking. Experimental measurements have been performed by tracking multiple objects.

2. RADIO TELESCOPE RT-32

The key applications of RT-32 are VLBI observations of ionosphere, participation in the European VLBI Network (EVN), radar-VLBI (investigation of radio-silent near-space objects, such as cosmic debris, asteroids), and single-dish solar observations. This kind of usage defines strict requirements for the whole drive system, mainly due to needs of fast switching between observational objects and accurate tracking of relatively fast objects.

RT-32 can rotate around azimuth (vertical) and altitude (horizontal) axes. Two motors drive the azimuth axis and the other two motors move the altitude axis. All the motors are driven in the current mode with the aid of electro-mechanical amplifiers. Angular positions on the both axes are measured using rotary encoders, angular velocities – with tachometers. Simplified telescope scheme is illustrated in Fig 1.

The main frequency range of the telescope is 1 – 12GHz. For this study, 5 GHz frequency has been used; therefore, RT-32 beam width is 7.8 arcmin. It has

been assumed that the antenna "sees" an observational object if it is at least 4 arcmin from the target, and that the antenna must be on track for at least 20 seconds in order to have viable output from the correlation software.

Technologically, the pointing accuracy of the RT-32 antenna is strictly limited to 20 arc sec, mainly due to a digital sampling error of the optical angular encoders from the period of 1960–1980. At the moment of paper submission, a large-scale renovation of RT-32 is taking place at VIRAC. After renovation in 2015, new azimuth sensors have specification of nominal resolution of »1.2 arc sec.

However, as it follows from the practice, the total pointing error usually reaches much higher values. Analysis of recent observation sessions (2008–2014) indicates that tracking accuracy is often limited by settling time, which for the existing RT-32 antenna drive system can reach ≈40 s and even more. These oscillations mainly happen during the target switching when the dish slows down from the "highway" angular velocities of approximately »10 deg/min to much slower pace of celestial bodies. The amplitude of these prolonged oscillations can be large enough to disturb the observation session – in fact settlement oscillations of the main mirror may disable VLBI observations for up to 70 % of total targets of EVN sessions. More targets could be tracked by suppression of oscillations after target switching.

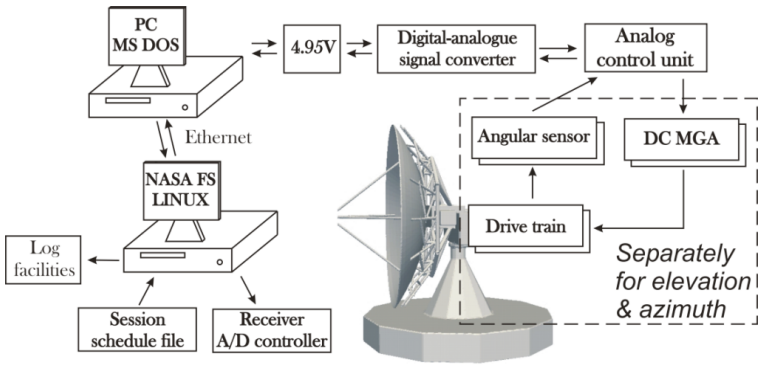

Fig. 1. Simplified scheme of RT-32 (in 2014), where NASA FS is NASA Field System, DC MGA is DC motor-generator amplifier.

2.1. Control System of RT-32

The radio telescope RT-32 is controlled by a PID controller. Such controllers are widely used in the antenna and radio telescope industry. The controller can be expressed mathematically as [4]:

$$u(t) = k_p e(t) + k_i \int_0^t e(\tau)\, d\tau + k_d \frac{de(t)}{dt}, \quad (1)$$

where *u(t)* is input signal of the plant (manipulated variable), *e(t)* is error signal defined as $e(t)=r(t)-y(t)$, *r(t)* is reference input signal, k_p is controller gain, k_i is integral gain and k_d is derivative gain. The process variables *y(t)* are signals from angular encoders (in *e*) and tachometers (in *de/dt*).

To obtain an optimal set of parameters k_p, k_d, and k_i that will give a stable operation of the RT-32 system, manual controller tuning has been performed during Sun and satellite observations. These parameters may differ for the cases of tracking, pointing and controlled movements (like switching from one celestial body to another).

The AC converter imposes a threshold limit of output voltage $|u|=u_0$ (where $u_0=4.95\ V$ is a control voltage), which breaks linearity of Eq. (1).

There are three modes of operation (separately for each axis) in the PID controller depending on a distance from the target. If the antenna is more than 3 degrees away from a target, the antenna is moved with maximum possible velocity. When the antenna reaches 3 degrees from the object trajectory, the PID controller takes over, but the integral part of the PID controller is enabled only when the antenna is 0.25 degrees from the trajectory of a targeted object.

The principal problem related to this approach is poor settling performance after a large move (see Fig. 2(a)).The integral sum starts accumulating when the controller is first switched on and continues to change as long as a controller error exists. If there is a difference between the desired and measured values, the resulting error will cause a continuing increase in the integral term.

In our case, the suppression of the integral windup is implemented with the help of an additional algorithm (PID+AA), which calculates a new tracking trajectory of an antenna (see Fig. 2(b)). A modelled trajectory starts at the initial position of the antenna and finishes at some point on the trajectory of the target. We would like to speculate that the algorithm can reduce oscillations of the antenna, because when the antenna is in a position where the PID controller takes over, the antenna control is no longer correcting errors between the current position and the desired position. Instead, it is now correcting errors between the current position and the provided trajectory. Because of the minimal differences, this results in a smoother deceleration, when the antenna reaches its targeted position.

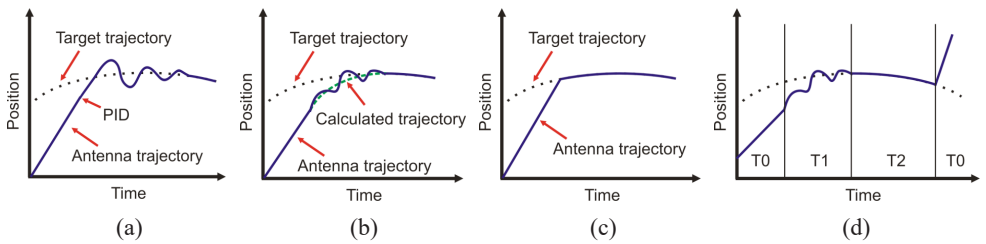

Fig. 2. Illustration of the initial RT-32 control (PID) with noteworthy oscillations (a); implemented approach for the suppression of the integral windup (b) using an additional algorithm (PID+AA); trajectory of an ideal plant and control (c). Time regions in target observation (d): the antenna moves at a maximum speed or acceleration, T0, the antenna reaches a target trajectory, T1, and the antenna tracks a target, T2.

We have assumed an ideal control and ideal plant which can move without any oscillations and immediately be on the trajectory when it is reached to get the qualitative estimation of algorithm efficiency (see Fig. 2(c)). Time and position when

the ideal system gets the target trajectory are defined using the maximum velocity of the antenna.

Observational time of a target can be divided into three time regions (see Fig. 2(d)): (1) a region where the antenna moves at a maximum speed or acceleration to reach a trajectory of the observational object, T0; (2) a region of corrections – pointing and settling time, T1; (3) a tracking region of a target, T2.

3. DYNAMICAL MODEL OF THE SERVO SYSTEM

To analyse fictive observation sessions and to study different control approaches and algorithms for antenna control, the dynamical model of RT-32 has been developed. Because of the RT-32 technical robustness (notable non-linearity and hysteresis of current amplifiers and engines, noisy encoders), it is a challenge to develop a dynamical model of this telescope servo system. The model which is in the acceptable agreement with the observed behaviour of RT-32 includes the drive system, second-order friction, and noise. Equations (2)–(3) describe the kinematics and dynamics of the model:

$$\dot{\alpha} = \int_{t_0}^{t_n} \ddot{\alpha} dt + \dot{\alpha_{t_0}}, \qquad \alpha = \int_{t_0}^{t_n} \dot{\alpha} dt + \alpha_{t_0}, \tag{2}$$

where $\dot{\alpha} = \omega$, and

$$\dot{\omega} = \frac{M_0}{\omega_s}\left[u_{ref} - \omega_{ref} + \kappa\omega_{ref} - \kappa\omega_{ref}^2 + \lambda f_g\right], \tag{3}$$

where M_0 is torque constant, $u_{ref}=u/u_0$, u is voltage, $w_{ref}=\omega/w_s$, w_s is maximum angular velocity, ω is angular velocity, λ and κ are friction constants, and η is noise. Gear friction f_g is:

$$f_g = \frac{d}{dt}\int_0^t v(t-\tau)e^{-\tau/\tau_0}d\tau. \tag{4}$$

DC motor-generator amplifier (DC MGA) is part of the model. Experimentally measured DC MGA transfer curve is shown in Fig. 3.

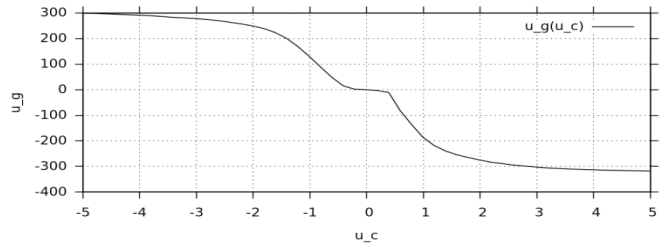

Fig. 3. Measured DC motor-generator amplifier transfer curve of the radio telescope RT-32.

The comparison of experimental and model values has shown that a magnetic hysteresis-like phenomenon has to be taken into account. The hysteresis is defined

by the following integral:

$$u_{mag} = \xi \int_0^t f(u_c, u_{mag}) \left|\frac{du_c}{d\tau}\right| d\tau, \tag{5}$$

where

$$f(u_c, u_{mag}) = \begin{cases} 0, if \ |u_c - u_{mag}| < 3.5 \\ 1, \ else \end{cases} \tag{6}$$

and u_c is voltage calculated by considering time delay and internal resistance of the system, ξ is a model constant.

4. POLYNOMIAL-BASED TRACKING ALGORITHM

The following happens in a standard VLBI tracking scenario. When a track command of RT-32 is called, the control system software uses an astronomical module to create a table, which describes the desired antenna position and the time when the antenna needs to be in the particular position to follow the body specified. The control algorithm then ensures the movement of the antenna between entries of a created table at a speed necessary to reach the next position described in this table. The algorithm automatically blends together subsequent moves so that the ending velocity and position of one move become the starting velocity and position for the next move.

To minimise the settling time introduced by the PID controller, a similar approach to [11] and [12] has been designed to move the antenna in a position to track objects.

During the study, a second-order polynomial has been inspected to define the antenna path in the hyperspace of two angles and time. However, in situations when the antenna's current position and targeted object position are very close and the antenna is moving slowly a second-order polynomial does not provide significant improvement. This can be explained by the fact that the tracking algorithm does not take the necessary acceleration of the antenna into account, when creating a trajectory for the desired object. For situations when antenna's motion is slow and the distance to the targeted object is small this results in trajectories that require antenna acceleration that exceeds system limitation.

Additional algorithm continuously checks the antenna position. When the antenna moves closer than 3 degrees from the source, it creates a trajectory using a third-order position polynomial (Eq. (7)), which the controller should employ for the antenna to reach its intended position.

$$x(t) = x_0 + \alpha\tau + \beta\tau^2 + \gamma\tau^3, \tag{7}$$

where $x(t)$ is antenna position at time t, x_0 is current antenna position and τ is time difference between t and t_0 which is current time. To find the coefficients α, β, and γ, a system of linear equations needs to be solved:

$$x(\Delta\tau) = x_1,\ x_1' = \alpha + 2\beta\Delta\tau + 3\gamma\Delta\tau^2,\ x_0' = \alpha, \tag{8}$$

where x_1 is coordinates of an object, x'_1 is velocity of this object, x'_0 is current velocity of the antenna and $\Delta\tau$ is time difference between current time (t_0) and time needed to reach the source trajectory (t_1).

All of the variables necessary to find α, β, and γ are known, except for time t_1 which is found in iterative way moving point x_1 until it is possible to create a trajectory, which leads the antenna without exceeding its maximum possible velocity.

A simple reach ability test is performed when a potential trajectory is calculated in order to check whether the antenna can make this trajectory without exceeding its maximum acceleration and velocity.

5. RESULTS AND DISCUSSION

To check the polynomial-based tracking algorithm, test observations have been performed. Several objects have been tracked. Logged observational data have been used as input to get model results. We have analysed five test cases that simulate real EVN sessions. In addition to the experiments with real antenna, the model antenna described in Section 3 has been used with even more EVN session motion schedules. For the same schedules the model appears to be sufficiently good to replace a real antenna. An example of a typical EVN session schedule with results of experiment and simulations is shown in Fig. 4(a).

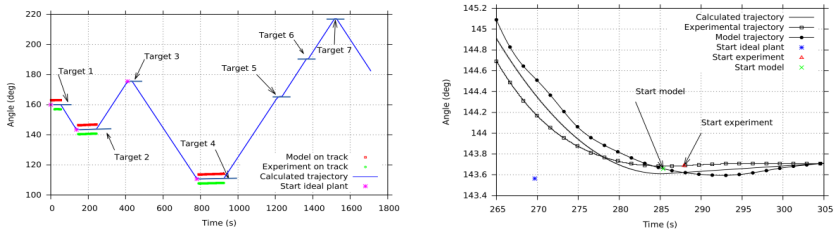

(a) (b)

Fig. 4. Example of EVN session with seven observational targets (a). Observational object trajectories are shown with horizontal lines. Comparison of an antenna trajectory during tracking using an ideal plant, experimental, and model results (b).

Time and position, when the ideal plant is on the source trajectory is marked with a star in Fig. 4(a). Time when a model and an experiment are on observational object trajectory is marked with a square (above theoretical trajectory) and circle (below theoretical trajectory), respectively. Both the modelled and experimental trajectories have not fulfilled conditions to observe Target 3; however, theoretically it should have been observed. There are three cases (Target 5, Target 6, and Target 7), where calculated observational time of the object is less than 20 seconds; therefore, it is assumed that objects have not been observed.

The effectiveness of the tracking algorithm has been calculated as the ratio of tracking time of controlled antenna to the tracking time of an "ideal" antenna. In both

cases antenna must be on trajectory of the object for at least 20 seconds before counting starts (for initial data collection needed for cross-correlation). For an "ideal" case we assume that the antenna (plant) reaches trajectory of the object trajectory (marked with a star in Fig. 4(b)) at a maximum hardware velocity and follows an absolute and stable tracking after.

Results of five test cases are summarised in Table 1. Results show that on average time (T0) spent for antenna movement between observational objects takes from 64 % (model and experiment) till 66 % (ideal plant) of all the time of a particular session. An "ideal" case has no pointing and settling time (T1); therefore, T0 is larger than in the model and experiment. Time (T1) is from 3 % till 9 % depending on the case (for model and experiment). On average, the efficiency of the controller is lower by 12 % when compared to an ideal plant (unreachable condition) while the experiment efficiency is lower by 14 %. In all cases when an ideal plant has not observed a target, it happened due to observational 20 second start-up limit discussed above. Model and experiment have not observed sources also due to large settling time (oscillations of the antenna).

Table1

Division of Normalized Time Regions of Different Observation Sessions

Cases	Type		T0	T1	T2	Targets (observed/ total)
Case 1	PID	Ideal	0.678	-	0.322	8/10
		Model	0.645	0.077	0.278	6/10
		Exp		0.090	0.265	6/10
Case 2	PID	Ideal	0.529	-	0.471	6/8
		Model	0.548	0.029	0.433	4/8
		Exp	0.567	0.057	0.377	3/8
Case 3	PID+AA	Ideal	0.607	-	0.393	6/8
		Model	0.569	0.061	0.370	6/8
		Exp		0.079	0.352	6/8
Case 4	PID+AA	Ideal	0.678	-	0.322	8/10
		Model	0.632	0.080	0.288	7/10
		Exp	0.619	0.072	0.309	8/10
Case 5	PID+AA	Ideal	0.809	-	0.191	4/7
		Model	0.817	0.030	0.153	3/7
		Exp		0.030	0.153	3/7

Both the experimental and modelling results show that an improved algorithm (PID+AA) that uses the 3rd-order polynomial and considers current antenna velocity when calculating a trajectory allows reaching a target sooner and consumes less time for pointing and settling than previously used methods (PID). As can be seen in examples provided in Table 2, the average value of time region T1 for a single target using only a PID controller is 60.95 s whereas using PID with an additional algorithm is 31.61 s.

Table 2

Average Value (in Seconds) of Correction Region T1 (Pointing and Settling Time) for Single Observational Target

Cases	Type	Average time of T1 for a single object (s)
Case 1	PID	57.73
Case 2	PID	64.17
Case 3	PID+AA	29.49
Case 4	PID+AA	39.51
Case 5	PID+AA	25.82

6. CONCLUSIONS

Smooth trajectory generation approach has been developed and applied to the existing PID controller of antenna. We have developed a dynamical model of servo system to be able to analyse more observation sessions with no need of use of expensive time of real antenna and to perform case studies by comparing various control algorithms. Despite mechanical robustness of the radio telescope RT-32, our telescope model results fit well with the experimental values.

Third-order polynomial-based trajectory generation algorithm has been worked out and tested. Test observations with RT-32 have been done to check the improved approach. Experimental and model results (as well as theoretical considerations) show that a 3rd-order polynomial trajectory generator ensures fewer oscillations of the antenna when moving from one object to another than relying only on switching on or off a basic PID control algorithm.

ACKNOWLEDGEMENTS

Research is presented as part of Project No. L-KC-11-0006, funded by the European Regional Development Fund.

REFERENCES

1. Gawronski, W., and Souccar, K. (2005). Control systems of the large millimeter telescope. *IEEE Antennas and Prop. Mag. 47* (4), 41–49.
2. Astrom, K.J, and Hagllund, T. (1995). *PID Controllers Theory, Design and Tuning*, 2nd ed. Instrument Society of America.
3. Ogata, K. (2002). *Modern Control Engineering,* 4th ed. New Jersey: Prentice Hall.
4. Astrom, K. J. and Murray, R. M. (2010). *Feedback Systems. An Introduction for Scientists and Engineers,* 2nd ed. Princeton, Oxford: Princeton University Press.
5. Peng, Y., Vrancic, D., and Hanus, R. (1996). Anti-windup, bumpless, and conditioned transfer techniques for PID controllers. *IEEE Control Systems*, *16* (4), 48–57.
6. Kanamori, M. (2013). Anti-windup adaptive tracking control for Euler-Lagrange systems with actuator saturation. In *3rd Int. Conf. on Instr. Control and Automation*, 28–30 August 2013 (pp. 216–221).
7. Mandarapu, S., Lolla, S., and Kumar, M.V.S. (2013). Digital PI controller using anti-wind-up mechanism for a speed controlled electric drive system. *Int. J. of Innovative Tech. and Exploring Eng. 3* (1), 239–242.

8. Hu, K., et al. (2013). Simulation and analysis of LQG controller in antenna control system. In *IEEE 4th Int. Conf. on Electronics Information and Emergency Communication*, 15–17 November 2013 (pp. 268–273).
9. Gawronski, W. (2001). Antenna control systems: from PI to H∞. *IEEE Antennas and Prop. Mag. 43* (1), 52–60.
10. Gawronski, W. (2002). *A Command Preprocessor for Antenna Motion without Overshoots*. Interplanetary Network Progress Report. Pasadena, California: Jet Propulsion Laboratory.
11. Smith, D.R., and Souccar K. (2008). A polynomial-based trajectory generator for improved telescope control. In *Proc. SPIE 7019, Advanced Software and Control for Astronomy II*.
12. Rivetta, C., Briegel, C. and Czarapata, P. (2000). Motion control design of the SDSS 2.5 mts telescope. In *Proc. SPIE 4004, Int. Soc. Opt. Eng. 2000*(pp. 212–222).

GLUDAS SEKOŠANAS TRJEKTORIJAS IZVEIDE LIELĀM ANTENĀM

S. Upnere, N. Jēkabsons, U. Locāns

K o p s a v i l k u m s

Antenu un teleskopu kontroles sistēmai jānodrošina precīza uzvadīšana un sekošana novērojamam objektam.

Vadīšanas precizitāti ietekmē gan antenas tehniskie parametri (maksimālais pārvietošanās ātrums un paātrinājums, motoru griezes moments utml.), gan izmantotie kontroles algoritmi.

Šajā publikācijā ir aprakstīts pilnveidots kontroles algoritms, kas uzlabo mehāniski robusta, liela radioteleskopa sekošanu vairākiem novērojamiem objektiem pēc kārtas. Lai samazinātu PID kontroliera izraisītas antenas oscilācijas laikā, kad tā sasniedz mērķa trajektoriju, pārvietojoties no viena pētāmā objekta uz citu, tiek izmantots papildus trešās kārtas polinoms, kas ļauj izveidot gludu uziešanu uz mērķa trajektorijas.

Radioteleskopa RT-32 dinamiskais modelis ir izveidots, lai analizētu novērojumu sesijas pirms to uzsākšanas, kā arī, lai novērtētu kontroles algoritmu efektivitāti. Uzlabotais kontroles algoritms tika pārbaudīts gan izmantojot reālus EVN novērojumu sesijas grafikus ar RT-32, gan radioteleskopa dinamisko modeli. Abos gadījumos rezultāti apstiprina, ka 3. kārtas polinoma izmantošana trajektorijas izveidē samazina antenas oscilācijas sasniedzot mērķa trajektoriju.

27.08.2015.